Journal of Pharmaceutical Analysis 9 (2019) 185–192

Contents lists available at ScienceDirect

Journal of Pharmaceutical Analysis

journal homepage: www.elsevier.com/locate/jpa

Original Article

Preparation of polypyrrole/nanosilica composite for solid-phase microextraction of bisphenol and phthalates migrated from containers to eye drops and injection solutions

Mehdi Ansari Dogaheh [a], Mansoureh Behzadi [b, *]

[a] Department of Pharmaceutics, Faculty of Pharmacy, Kerman Medical Science University, Kerman, Iran
[b] Department of Chemistry, Faculty of Science, Shahid Bahonar University of Kerman, Kerman, Iran

ARTICLE INFO

Article history:
Received 12 August 2018
Received in revised form
12 March 2019
Accepted 12 March 2019
Available online 15 March 2019

Keywords:
Solid-phase microextraction
Gas chromatography-mass spectrometry
Polyphosphate-doped polypyrrole
Nanosilica
Phthalates
Bisphenol A

ABSTRACT

This paper describes the electrodeposition of polyphosphate-doped polypyrrole/nanosilica nanocomposite coating on steel wire for direct solid-phase microextraction of bisphenol A and five phthalates. We optimized influencing parameters on the extraction efficiency and morphology of the nanocomposite such as deposition potential, concentration of pyrrole and polyphosphate, deposition time and the nanosilica amount. Under the optimized conditions, characterization of the nanocomposite was investigated by scanning electron microscopy and Fourier transform infra-red spectroscopy. Also, the factors related to the solid-phase microextraction method including desorption temperature and time, extraction temperature and time, ionic strength and pH were studied in detail. Subsequently, the proposed method was validated by gas chromatography-mass spectrometry by thermal desorption and acceptable figures of merit were obtained. The linearity of the calibration curves was between 0.01 and 50 ng/mL with acceptable correlation coefficients (0.9956–0.9987) and limits of detection were in the range 0.002–0.01 ng/mL. Relative standard deviations in terms of intra-day and inter-day by five replicate analyses from aqueous solutions containing 0.1 ng/mL of target analytes were in the range 3.3%–5.4% and 5%–7.1%, respectively. Fiber-to-fiber reproducibilities were measured for three different fibers prepared in the same conditions and the results were between 7.3% and 9.8%. Also, extraction recoveries at two different concentrations were ≥96%. Finally, the suitability of the proposed method was demonstrated through its application to the analysis of some eye drops and injection solutions.

1. Introduction

Endocrine disruptors including alkylphenols, polybrominated diphenyl ethers, parabens, bisphenols and phthalate esters are a class of chemicals used in a wide range of materials found in daily life [1]. These environmental estrogens combine with estrogen receptors in womb, pituitary and other organs via simulating the activities of endocrine hormones and interfere with the normal functions of endocrine system, leading to infertility, mutation, tumor and hypogenesis of reproductive system [2,3].

Bisphenol A (BPA) is a raw chemical intermediate in the production of epoxy adhesives, polycarbonate plastics, white dental fillings and food can lining [4–6]. Dialkyl or alkyl aryl esters of 1,2-benzenedicarboxylic acid or phthalate esters (PEs) are widely found in industrial applications. High molecular weight PEs are used as plasticizers in polymers to improve their flexibility, extensibility and durability, and low molecular weight PEs are used in personal care products as solvents or carriers [7]. These chemicals bind physically to the polymers, so they can easily migrate from plastic containers to surrounding medium. Because of this, they are ubiquitous in aquatic environments. Therefore, it is necessary to develop more researches in extraction and quantitative analysis of these pollutants.

Solid-phase microextraction (SPME) is a miniaturized solvent free process that integrates sampling, extraction, preconcentration and introduction into one step. Since fused silica SPME fibers are fragile, metal wires with high mechanical stability have been developed for daily applications in recent years. Various metallic substrates such as aluminum [8], copper [9], platinum [10], porous silver [11] and stainless steel [12,13] are coated with different types

Peer review under responsibility of Xi'an Jiaotong University.
* Corresponding author.
E-mail address: m.behzadi85@gmail.com (M. Behzadi).

https://doi.org/10.1016/j.jpha.2019.03.006

of sorbents [10,14–17]. Many types of organic polymers such as conducting and non-conducting polymers are the most widely sorbents used as coating on metallic supports in SPME [18–20]. Electroactivity, hydrophobicity, ion-exchange property, polar functional groups along with hydrogen bonding and π-π interaction are multiple functional properties of organic polymers that attract great attention in the field of extraction of organic compounds [21]. Also, these polymers can be polymerized conveniently with oxidation reactions from an aqueous solution containing monomers and dopant ions. Among a wide range of coating technique including sol-gel [22], chemical corrosion [23], direct pasting and pasting with adhesives [24,25], electrodeposition has attracted lots of attention due to the control of the coating film thickness and feasibility [26].

Polymeric nanocomposites are composed of a polymer matrix incorporating various reinforcement agents with at least one dimension in the nanoscale [27–30]. There is a strong interfacial interaction between polymer network and nanoreinforcements at higher loading and minimum aggregation. The bulk physical properties of polymer nanocomposites are shown to be superior to the pure polymer matrix [31]. Polypyrrole (Ppy) and its derivatives are the most frequently studied polymers due to their good environmental and thermal stabilities and facile synthesis [32]. They have many applications in electronic devices, chemical sensors and coating [33–35]. In general, the properties of these polymers are strongly dependent on the type and concentration of dopant [36]. Sodium polyphosphate is an anionic surfactant that can be used as a dopant in polymerization process. Indeed, incorporating such an immobilized and large polymeric surfactant into polymer matrix increases thermal stability of the polymer in an inert atmosphere [37]. Silica nanoparticles have many mechanical and structural properties such as excellent thermal stability, nontoxicity, chemical inertness and optical transparency that make them suitable as nanoreinforcement to incorporate into the polymer network [38]. On the other hand, polyphosphate and nanosilica increase the polarity of the nanocomposite, which is suitable for extraction of organic compounds with high polarity.

In this study, nanosilica and polyphosphate were successfully incorporate into the polypyrrole matrix to strengthen and improve the chemical properties of the polymer as a new coating in SPME. Then, BPA and PEs leached from some injection solution bags and eye drops containers were determined as model analytes for evaluating the extraction ability of this nanocomposite.

2. Experimental

2.1. Reagents

Bisphenol A (≥99%) was obtained from Sigma-Aldrich (Milwaukee, WI, USA). Diethyl phthalate (DEP), di-isobutyl phthalate (DIBP), dibutyl phthalate (DBP), benzyl butyl phthalate (BzBP) and bis-2-ethylhexyl phthalate (DEHP) were purchased from Merck (Darmstadt, Germany). The stock solution of these compounds was prepared in methanol (HPLC grade) and stored at 4 °C. Working solutions were prepared daily in double distilled water from the mixed stock solution. Pyrrole (>97% pure) was purchased from Merck (Darmstadt, Germany) and distilled under N_2 pressure for more purification and stored in darkness before use. The silica nanoparticles (12–50 nm diameter) were bought from Degussa Company (Darmstadt, Germany). Sodium chloride (analytical grade) and sodium polyphosphate (analytical grade) were obtained from Fluka (Buchs, Switzerland).

2.2. Apparatus

Separation and quantification of BPA and PEs were carried out using an Agilent 7890C gas chromatograph (Agilent Technologies, CA, USA) equipped with a split/splitless injector and coupled to a 5975C mass spectrometer with a quadrupole mass analyzer. The separation column was a 30 m × 0.25 mm i.d. fused-silica capillary column coated with 0.25 μm film of DB-5 (Agilent-J&W Scientific, Santa Clara, USA). Helium was used as carrier gas at a constant flow of 1.0 mL/min. Automatic injection of 1.0 μL sample was conducted at the splitless mode. The injection temperature was 280 °C. The column temperature was initiated at 100 °C for 1 min and then increased to 170 °C at a rate of 20 °C/min and then reached at 270 °C at 15 °C/min and finally kept at this temperature for 10 min. The analysis was conducted in a selected ion monitoring (SIM) mode and each analyte was quantified based on peak areas. The ions with *m*/*z* 149 (DEP, DIBP, DBP, BBP), *m*/*z* 167 (DEHP) and *m*/*z* 357 (BPA) were selected for quantification. Also, the ions with *m*/*z* 177, 205, 223, 238, 279 and 372 were used as confirmed ions for DEP, DIBP, DBP, BBP, DEHP and BPA, respectively.

The home-made SPME device consisted of a 25 gauge, 10 cm stainless steel spinal needle (Dr. Japan Co., Tokyo, Japan), embedded in a 6.0 cm hollow metal tubing for protection, and fitted at one end with a metal fitting containing a piece of rubber septum. A piece of steel wire (20 cm × 0.3 mm) passing through the septum acted as the SPME fiber. One end of the fiber was attached to a cap and 3.5 cm of the other end was coated with a thin film of the synthesized nanocomposite. Electrochemical polymerization of pyrrole was carried out with a Behpajuh potentiostat/galvanostat, model BHP 2061-C (Esfahan, Iran). Steel wire (type 302, 0.3 mm O.D.) used as the working electrode was obtained from American Orthodontics (WI, USA). The Ag/AgCl reference electrode and the Pt counter electrode used in the electrochemical process were from Azar Electrode Co., Urmieh, Iran. The scanning electron micrographs of the nanocomposite surface were obtained using a Hitachi S4160 scanning electron microscope (Tokyo, Japan). FTIR spectra were recorded by a Tensor 27 FT-IR spectrometer from Brucker (Ettlingen, Germany). Only glassware was used to avoid the possible contamination due to BPA and PEs deriving from plastics.

2.3. Preparation of the coating

First, 0.01 g nanosilica was dissolved in 5 mL of pyrrole monomer solution (0.1 M) containing 10% sodium polyphosphate and stirred under sonication for 15 min to obtain a homogenous solution. On the other, the surface of a stainless steel wire (3.5 cm in length) was scrubbed by a sand paper, washed in acetone and water several times while sonicated and then dried in an oven at 100 °C for 1 h. This was used as working electrode. The nanocomposite coating was directly deposited on the working electrode from the homogenous solution by applying a constant potential of 1.2 V for 1250 s at room temperature. After polymerization, the synthesized SPME fiber was assembled in the home-made SPME device, heated at 100 °C for 1 h in an oven, and finally conditioned at 300 °C for 3 h in the GC injector port under a helium atmosphere. The film thickness of the final coating prepared under these conditions was determined to be 50 μm.

2.4. The microextraction process

The SPME process was performed by placing 10.0 mL samples into a 15.0 mL sample vial capped with a septum. Magnetic stirring with a stirring bar was used to agitate the sample solution.

Extractions were carried out by exposing a 3.5 cm length of the nanocomposite-coated fiber to the sample solution of BPA and PEs (pH = 7). The extraction temperature (45 °C) was adjusted by placing the extraction vial in a water bath placed on the magnetic stirrer for 40 min. After extraction, the fiber was withdrawn into the needle, removed from the sample vial and immediately introduced into the GC injector port for thermal desorption (280 °C for 5 min).

3. Results and discussion

3.1. The coating optimization

Optimization of the coating conditions such as applying potential, deposition time, concentration of pyrrole, concentration of polyphosphate and nanosilica amount are required. The conventional optimization approach is based on one-factor-at-a-time experiments.

For investigating the effect of potential on the extraction efficiencies of the target analytes, a range of 0.7–1.8 V was applied to 0.1 M pyrrole solution containing 10% (w/v) polyphosphate and 0.005 g nanosilica for 1000 s. According to Fig. 1A, the use of 1.2 V provides the highest peak areas and therefore this value was selected as the optimum voltage. The deposition time of polymerization is another important parameter that must be studied. While a constant potential of 1.2 V, a time range of 500–1750 s in a 0.1 M pyrrole solution containing 10% (w/v) polyphosphate and 0.005 g nanosilica was investigated. By increasing the deposition time, the film thickness increased which led to lower surface area and resulted in a decrease of extraction efficiency. Finally 1250 s was found as the optimum value (Fig. 1B). Here, the monomer and the polyphosphate concentrations varied from 0.025 to 0.20 M and 1%–20% (w/v), respectively. It was observed that at high polyphosphate concentration, the coating nanocomposite would separate from the steel surface. Indeed, adhesion decreased with increasing concentrations of the polyphosphate and the lifetime of the coated fiber reduced. The highest efficiencies were obtained at 0.1 M pyrrole and 10% (w/v) polyphosphate (Fig. 1C). The use of nanosilica in polypyrrole structure caused the enhancement of surface area and porosity of the nanocomposite and improved extraction efficiency. For investigating the role of the nanosilica in the synthesized nanocomposite and subsequently in the extraction process, different amounts of nanosilica were added to 5 mL of the 0.1 M pyrrole and 10% (w/v) polyphosphate solution and polymerization was done under optimum potential and time. According to Fig. 1D, 0.01 g nanosilica was chosen for subsequent experiments.

3.2. Coating characterization

The surface characteristics of the synthesised nanocomposite coating were investigated by SEM. The micrographs of the silica nanoparticles, polyphosphate-doped poypyrrole and polyphosphate-doped polypyrrole/nanosilica composite fiber coating are shown in Figs. 2A–F. It indicates that the nanocomposite had a porous and non-smooth structure in comparison with the polyphosphate-doped poypyrrole film. That is for incorporating the nanosilica to the nanocomposite and this results in increasing the extraction efficiency of the nanocomposite compared with polyphosphate-doped poypyrrole composite. The FT-IR spectra of the nanosilica and the nanocomposite are showed

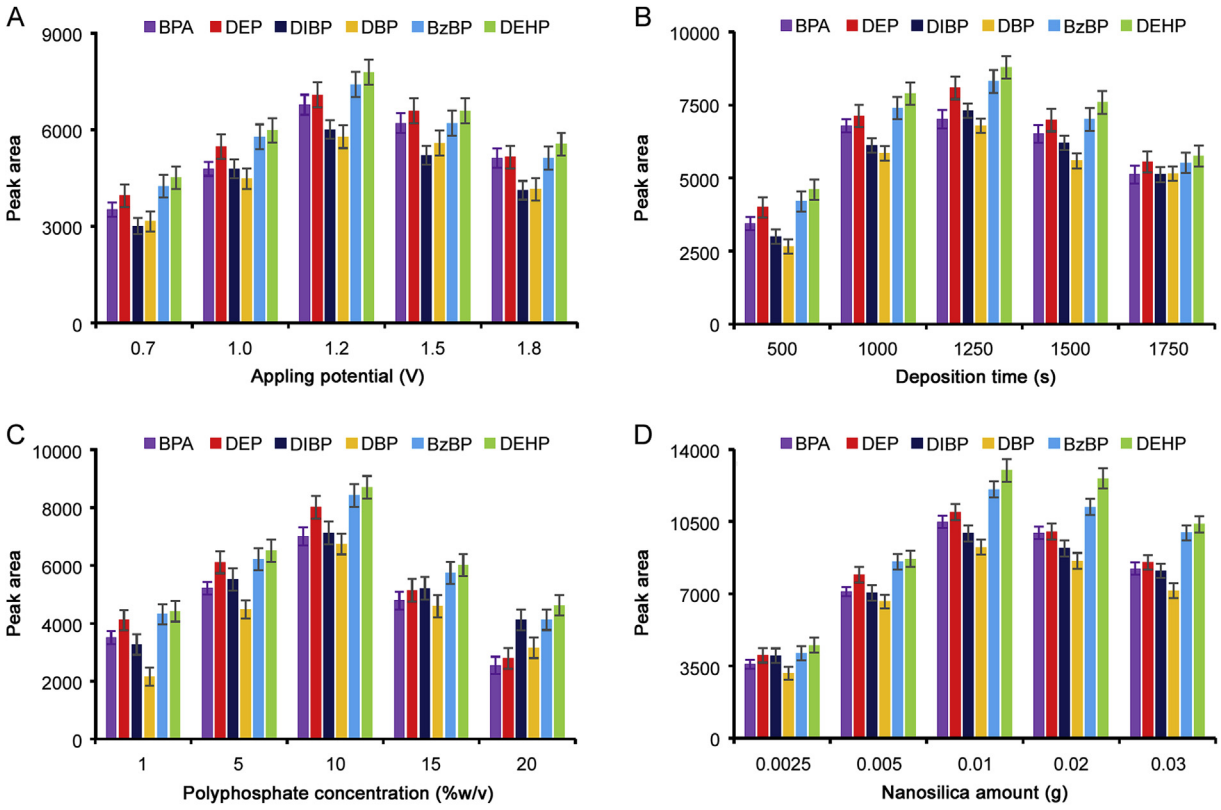

Fig. 1. Effect of coating parameters on the extraction efficiency. (A) applied potential, while the concentration of pyrrole, polyphosphate and nanosilica was 0.1 M, 10% (w/v) and 0.005 g, deposition time = 1000 s, (B) deposition time, while the concentration of pyrrole, polyphosphate and nanosilica was 0.1 M, 10% (w/v) and 0.005 g, applied potential = 1.2 V, (C) polyphosphate concentration, while the concentration of pyrrole and nanosilica was 0.1 M and 0.005 g, applied potential = 1.2 V, deposition time = 1250 s and (D) nanosilica amount, while the concentration of pyrrole and polyphosphate was 0.1 M and 10% (w/v), applied potential = 1.2 V, deposition time = 1250 ($n = 3$).

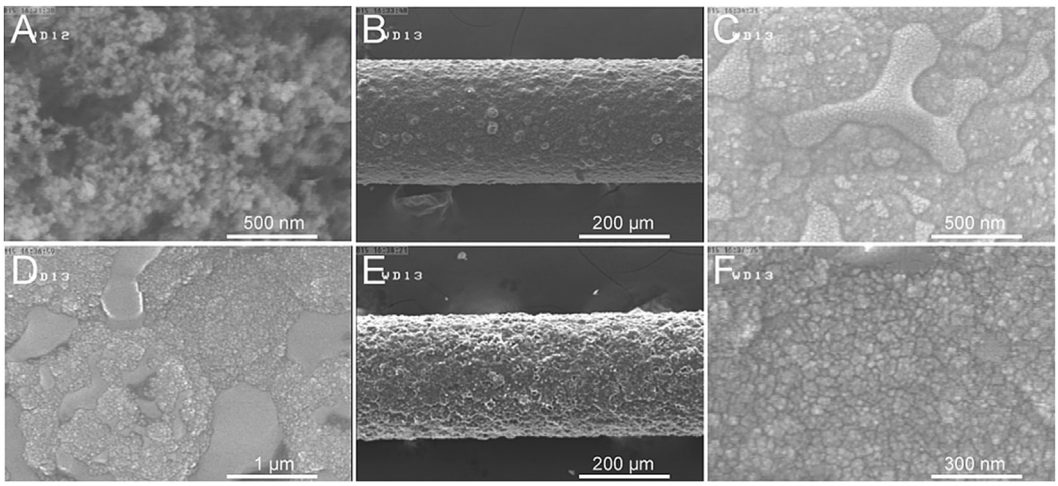

Fig. 2. Scanning electron micrograph images of (A) nanosilica with magnification 60,000 ×, (B & C) polyphosphate-doped polypyrrole composite film with magnification 150 × and 60,000 ×, (D, E & F) polyphosphate-doped polypyrrole/nanosilica nanocomposite with magnification 150 ×, 30,000 × and 100,000 ×; while the nanocomposite is in the optimized conditions.

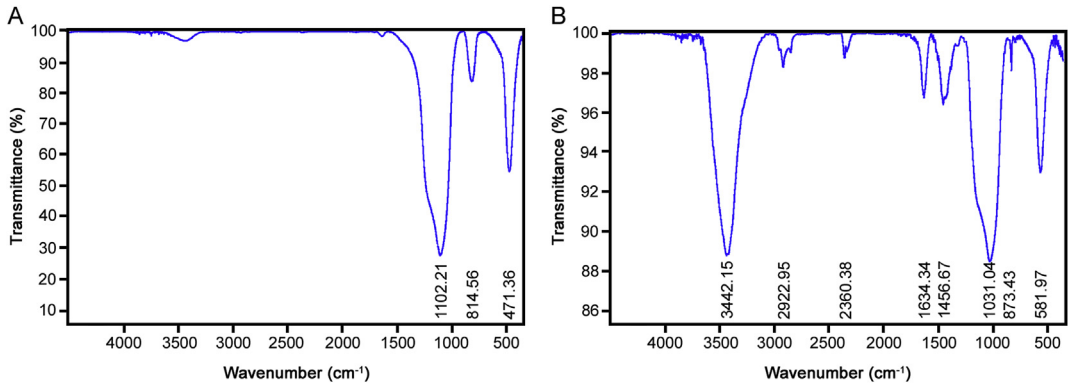

Fig. 3. FT-IR spectrum of (A) nanosilica and (B) polyphosphate-doped polypyrrole/nanosilica nanocomposite, while the nanocomposite is in the optimized conditions.

in Figs. 3A and B. In spectrum of the nanosilica, the peaks at 471.36 cm^{-1} and 814.56 cm^{-1} correspond to the Si–O out of plane deformation and bending, respectively. Also, the absorption band at 1102.21 cm^{-1} is assigned to the Si–O–Si stretching vibrations. On the other hand, the spectrum of the nanocomposite exhibits the absorption peaks which are attributed to the presence of SiO_2 in the composite. In addition, the peaks at 1456.67 cm^{-1} and 1634.34 cm^{-1} can be assigned to typical polypyrrole ring vibrations (C=C and =C–H). The absorption bands at 2800–3000 cm^{-1} correspond to the C–H stretching vibrations and the bands at 3000–3600 cm^{-1} are attributed to N–H stretching vibrations of PPY.

The stability of the prepared fiber was determined by using a fiber several times and investigating the extraction recovery. The experiment showed that this fiber could be used almost 80 times and after that the extraction recovery decreased ≤85%. Also, this experiment was done fiber-to-fiber ($n = 3$) and this value (80 times) was obtained.

3.3. Extraction optimization

To evaluate the potency of new nanocomposite in extraction of BPA and PEs from aqueous samples, different factors were considered.

Both desorption temperature and time utilized in SPME-GC method should be taken into account. In order to avoid carry over, the highest possible desorption temperature should be used without damaging the nanocomposite coating. For experimental analysis, the desorption temperature and time were changed within a range of 200–300 °C and 1–15 min, respectively. The results indicated that 280 °C and 5 min were sufficient to achieve the complete desorption (Figs. 4A and B).

SPME is a technique based on the equilibrium between the concentration of the analytes in the sample solution and those adsorbed by the fiber coating. To determine the acceptable time in this experiment, the nanocomposite coating was exposed to the sample solution containing the target analytes for 10–60 min and the responses are demonstrated in Fig. 5A. Considering the obtained peak areas, a gentle increase was observed up to 40 min and then the results for all analytes remained constant. Thus, 40 min was used as the optimum value.

The temperature has a considerable and diverse effect on the extraction process. An increase in temperature causes increase of the diffusion coefficient in water and subsequently shorter extraction time. On the other side, the distribution constant decreases at higher temperature because of the exothermic process of the adsorption. Also, elevated temperature leads to transfer of the analytes into the headspace due to the higher vapor pressure and since in this work, SPME process was direct, this transfer is not desirable. With these considerations, a temperature range of

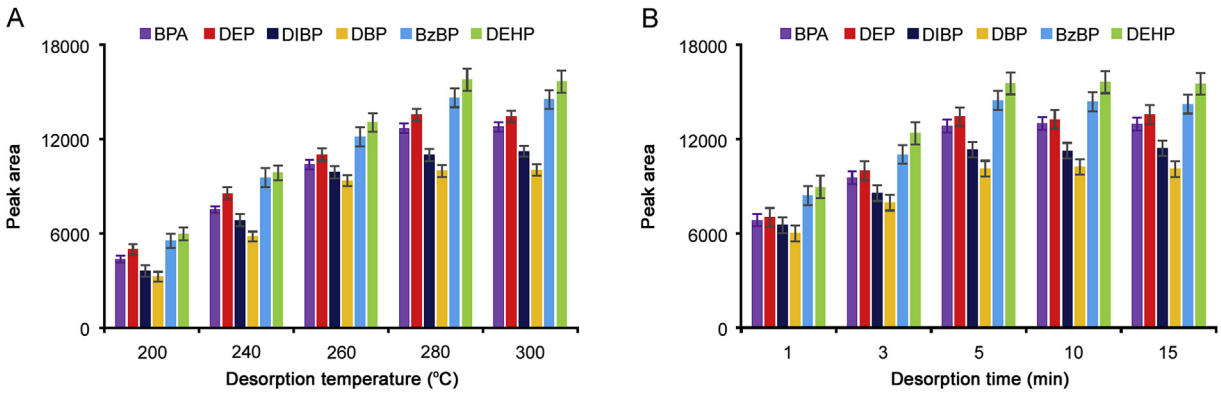

Fig. 4. Effect of desorption parameters on the extraction efficiency. (A) Desorption temperature and (B) desorption time, while the nanocomposite is in the optimized conditions, $n = 3$.

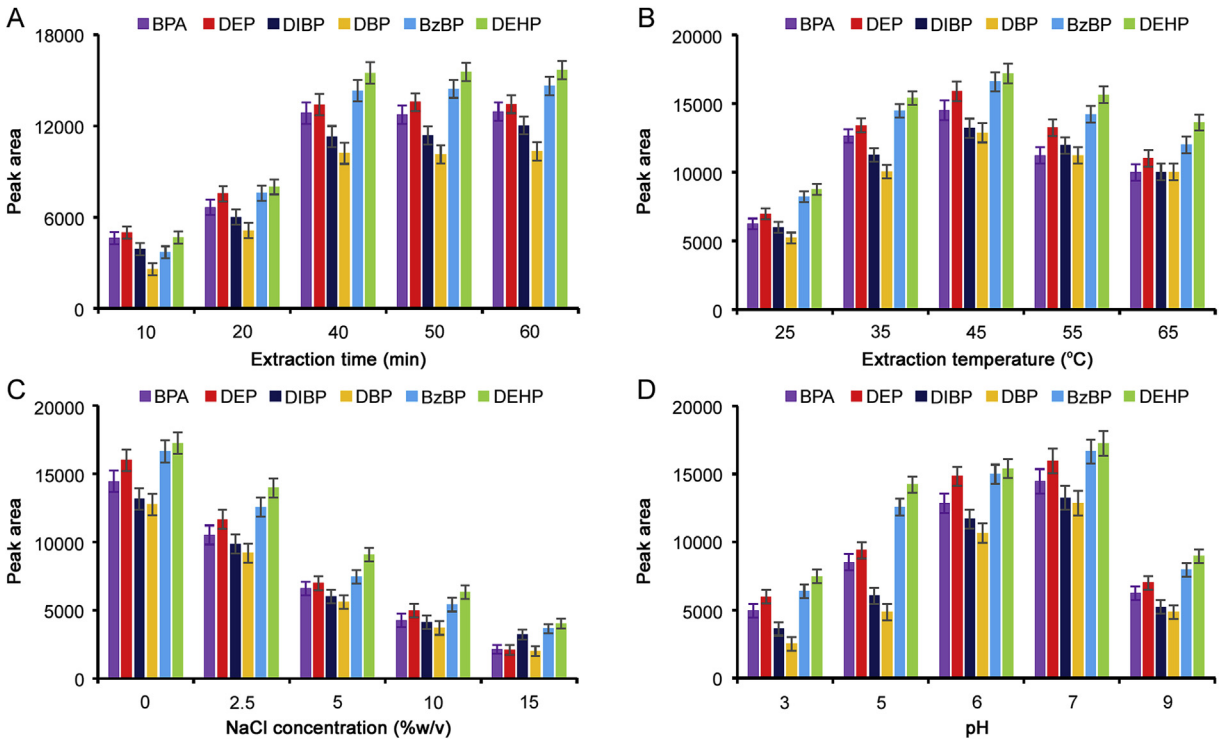

Fig. 5. Effect of extraction parameters on the extraction efficiency. (A) Extraction time, while extraction temperature = 35 °C, NaCl concentration = 2.5%, pH = 6, (B) extraction temperature, while extraction time = 45 min, NaCl concentration = 2.5%, pH = 6, (C) NaCl concentration while extraction time = 45 min, extraction temperature = 35 °C, pH = 6 and (D) pH, while extraction time = 45 min, extraction temperature = 35 °C, NaCl concentration = 0%; $n = 3$.

25–65 °C was applied to investigate the extraction temperature effect. As Fig. 5B shows, the peak areas were enhanced while temperature was raised up and reached at a maximum level at 45 °C and a decrease in peak areas was observed when temperature was further increased. Therefore, 45 °C was selected for the rest of experiments.

The effect of salt addition on the extraction efficiency was also studied by increasing an inorganic salt to the aqueous sample. Usually, the solubility of organic solute decreases with increased salt amount and consequently, the extraction efficiencies increased. In this study, the concentration of sodium chloride ranged from 0.0 to 15% (w/v) while the extraction temperature and time were kept at 45 °C and 40 min, respectively. It was observed that the addition of salt decreased the extraction efficiency of all target analytes due to the enhancement in solution viscosity (Fig. 5C). Hence, salt was removed from this extraction process.

In the present work, the effect of pH was studied at several levels of 3.0, 5.0, 6.0, 7.0 and 9.0. It was found that maximum extraction efficiencies were achieved at pH = 7 (Fig. 5D). While at other pH values, the extraction efficiencies were lower. Apparently, in both acidic and alkaline solutions, the analytes were unstable. Thus, in subsequent experiments the pH of water sample was adjusted at 7.

3.4. Method validation

The parameters related to the figures of merit for the optimized method were evaluated and the results concerning linear range (LR), limit of detection (LOD) and precision are presented in Table 1. The linearity of the curve was investigated using a wide range of

Table 1
Analytical figures of merit (limits of detection (LOD), linear ranges (LR), relative standard deviations (RSD)) and the extraction recoveries of the present work under the optimized conditions.

Compound	LOD	LR	Recovery (%) at different concentrations		RSD % (0.1 ng/mL)		
			0.1 ng/mL	1.0 ng/mL	Intra-day ($n=5$)	Inter-day ($n=5$)	Fiber-to-fiber ($n=3$)
BPA	0.01	0.05–50	98	96	4.3	6.1	8.5
DEP	0.005	0.01–50	101	99	5.1	6.6	9.1
DIBP	0.005	0.01–50	99	100	3.3	5.0	7.3
DBP	0.003	0.01–50	96	97	5.4	7.1	9.8
BBP	0.003	0.01–50	100	98	3.8	5.6	7.7
DEHP	0.002	0.01–50	105	101	4.9	6.3	8.9

concentration and an acceptable correlation coefficient was obtained for each analyte. In addition, LOD was calculated on the basis of S/N = 3 ratio and limit of quantification (LOQ) was considered as the lowest point of the calibration curve. The precision in terms of the intra-day and inter-day relative standard deviation (RSD%) was determined by five replicate analyses from aqueous solutions containing 0.1 ng/mL of target analytes. Also, the reproducibility of the fiber production expressed as the fiber-to-fiber reproducibility was measured for three different fibers, preparation under the same condition at 0.1 ng/mL.

The results presented in Table 2 indicate that the nanocomposite applied in the direct SPME-GC method has comparable analytical performance and extraction time and better extraction recovery in compared with other similar papers [39–44].

3.5. Analysis of real samples

Three kinds of eye drops (Chloramphenicol 0.5%, Betamethasone 0.1% and Naphazoline hydrochloride ophthalmic solution) and five kinds of intravenous injection solutions such as normal saline (0.9% sodium chloride solution), dextrose saline (5% glucose monohydrate and 0.9% sodium chloride solution), dextrose (10% glucose solution), Ringer's (sodium chloride, potassium chloride, calcium chloride and sodium bicarbonate) in plastic containers and dextrose 50% solution in glass container were purchased from a local pharmacy. The SPME process was performed under the optimum conditions by placing 10.0 mL of each real sample (pH = 7) into sample vial directly without any pretreatment. As shown in Table 3, some BPA and PEs were detected in these samples in plastic containers while they were not detected in dextrose 50% solution in glass container. Furthermore, the experiments showed that the PEs concentration tended to be high in the intravenous injection solutions which have longer storage periods. The extraction recovery is an important point to the evaluation of the ability of nanocomposite in the preconcentration and separation step. For this purpose, the extraction recovery was investigated at different concentrations and the results showed that the recoveries of BPA and PEs spiked to dextrose 50% solution were above 95% (Table 1). The chromatograms of chloramphenicol 0.5% eye drops, dextrose 10% injection solution, Ringer's injection solution and a mix standard sample spiked to dextrose 50% injection solution are indicated as Fig. 6.

4. Conclusion

In this work, a robust and reliable analytical method for the simultaneous determination of six endocrine disruptors (bisphenol A and five phthalate esters) in a single chromatographic run has

Table 2
Comparison of the extraction time (ET), recovery, linear range (LR), LOD and RSD of the present work with other works under the optimized conditions.

Item	Parameter	Present work	Ref.					
			[39]	[40]	[41]	[42]	[43]	[44]
Matrix		Injection solution	Waste water	Bottled water	Blood-seawater	Meat	Soil	Human urine
ET (min)		40	60	60	20	30	–	–
Recovery (%)		≥96	≥95	–	≥74	≥95	≥70	≥74
Compound								
BPA	LR (ng/mL)	0.05–50	0.15–5	–	2.0–100	–	1.0–50	–
	LOD (ng/mL)	0.01	0.05	–	0.096	–	0.13	–
	RSD (%)	4.3(0.1)	4.2(0.5)	–	5.0	–	3.0	–
DEA	LR (ng/mL)	0.1–50	0.025–0.5	0.2–20	1.0–100	0.26–4.07	–	20–500
	LOD (ng/mL)	0.005	0.01	0.049	0.15	0.13	–	7.86
	RSD (%)	5.1(0.1)	3.7(0.5)	1.38(1.5)	4.5	7(0.2)	–	1.49
DIBP	LR (ng/mL)	0.01–50	–	0.1–20	–	0.07–2.02	–	20–500
	LOD (ng/mL)	0.005	–	0.064	–	0.02	–	0.63
	RSD (%)	3.3(0.1)	–	3.62(1.5)	–	19(0.2)	–	1.82
DBP	LR (ng/mL)	0.01–50	0.3–5	0.1–26	1.0–100	0.07–4.05	–	20–500
	LOD (ng/mL)	0.003	0.12	0.066	0.004	0.01	–	3.25
	RSD (%)	5.4(0.1)	5.01(1.5)	5.01(1.5)	1.0	9(0.2)	–	2.72
BBP	LR (ng/mL)	0.01–50	0.4–5	0.1–20	1–100	0.26–4.12	–	20–500
	LOD (ng/mL)	0.003	0.15	0.085	0.1	0.18	–	7.18
	RSD (%)	3.8(0.1)	–	17.14(1.5)	3.3	16(0.2)	–	1.59
DEHP	LR (ng/mL)	0.01–50	0.3–5	0.1–20	–	0.13–4.11	–	20–500
	LOD (ng/mL)	0.002	0.13	0.049	–	0.08	–	0.36
	RSD (%)	4.9(0.1)	–	17.24(1.5)	–	16(0.2)	–	2.53

All the concentrations indicated in parenthesis are in ng/mL.

Table 3
Determination of BPA and PEs in real samples (placing 10.0 mL of each real sample with pH = 7 into sample via directly, without any pretreatment studied under the optimized extraction conditions).

Real sample	Concentration (ng/mL)					
	BPA	DEP	DIBP	DBP	BBP	DEHP
Eye drops A	ND	ND	8.8 ± 0.58	5.9 ± 0.45	ND	4.1 ± 0.30
Eye drops B	0.30 ± 0.20	ND	ND	8.6 ± 0.85	ND	3.4 ± 0.37
Eye drops C	0.50 ± 0.25	ND	ND	6.3 ± 0.90	ND	ND
Injection solution A	ND	3.2 ± 0.15	ND	0.90 ± 0.22	ND	ND
Injection solution B	3.2 ± 0.29	ND	ND	ND	ND	4.1 ± 0.30
Injection solution C	5.2 ± 0.32	ND	8.9 ± 1.0	ND	ND	5.6 ± 0.41
Injection solution D	0.80 ± 0.20	4.4 ± 0.36	ND	9.3 ± 1.2	ND	6.2 ± 0.52
Injection solution E	ND	ND	ND	ND	ND	ND

Eye drops A: Chloramphenicol 0.5%, Eye drops B: Betamethasone 0.1%, Eye drops C: Naphazoline hydrochloride ophthalmic solution.
Injection solution A: Normal saline, Injection solution B: Dextrose saline, Injection solution C: Dextrose 10% solution, Injection solution D: Ringer's solution, Injection solution E: Dextrose 50% solution.
ND: Not detected.

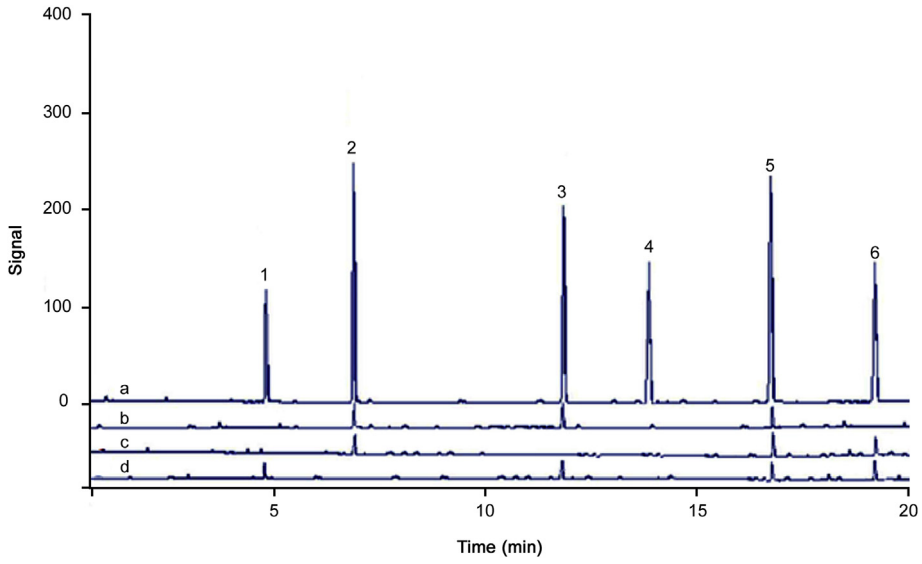

Fig. 6. The chromatograms of (A) standard sample in dextrose 50% solution as matrix, (B) eye drops A, (C) injection solution C and (D) injection solution D (1:DEP, 2:DIBP, 3:DBP, 4: BBP, 5: DEHP & 6: BPA).

been developed. The extraction method is based on solid-phase microextraction with a new home-made nanocomposite fiber coating that has better thermal, mechanical and chemical stability compared with conventional fibers. On the other hand, by incorporating nanosilica in polypyrrole-polyphosphate network, the specific surface area and active sites of the nanocomposite are enhanced through π-π interaction between analytes and the coating, and provide an appropriate platform for efficient adsorption and separation. The analytical characteristics of the developed methods are satisfactory for all the analytes investigated. Eventually, the proposed method has been successfully applied into the real sample detection and determination.

Acknowledgments

We gratefully acknowledge financial support of Department of Pharmaceutics, Faculty of Pharmacy, Kerman Medical Science University.

Conflicts of interest

The authors declare that there are no conflicts of interest.

Appendix A. Supplementary data

Supplementary data to this article can be found online at https://doi.org/10.1016/j.jpha.2019.03.006.

References

[1] C. Monneret, What is an endocrine disruptor? C.R. Biol. 340 (2017) 403–405.
[2] M. Giulivo, M.L. Alda, E. Capri, et al., Human exposure to endocrine disrupting compounds: their role in reproductive systems, metabolic syndrome and breast cancer. A review, Environ. Res. 151 (2016) 251–264.
[3] M. Kampa, G. Notas, E. Castanas, Natural extranuclear androgen receptor ligands as endocrine disruptors of cancer cell growth, Mol. Cell. Endocrinol. 457 (2017) 43–48.
[4] J.M.L. Reis, F.C. Amorim, A.H.M.F.T. da Silva, et al., Influence of temperature on the behavior of DGEBA (bisphenol A diglycidyl ether) epoxy adhesive, Int. J. Adhes. Adhes. 58 (2015) 88–92.
[5] M.L. Spagnuolo, F. Marini, L.A. Sarabia, et al., Migration test of Bisphenol A from polycarbonate cups using excitation-emission fluorescence data with parallel factor analysis, Talanta 167 (2017) 367–378.
[6] T.L.L. Berge, G.B. Lygre, B.A.G. Jönsson, et al., Bisphenol A concentration in human saliva related to dental polymer-based fillings, Clin. Oral Investig. 21 (2017) 2561–2568.
[7] P. Viñas, N. Campillo, M. Pastor-Belda, et al., Determination of phthalate esters in cleaning and personal care products by dispersive liquid–liquid microextraction and liquid chromatography–tandem mass spectrometry, J. Chromatogr. A 1376 (2015) 18–25.
[8] M.M. Abolghasemi, V. Yousefi, M. Piryaei, Fabrication of a hierarchical dodecyl

sulfate-layered double hydroxide nanocomposite on porous aluminum wire as an efficient coating for solid-phase microextraction of phenols, Microchim. Acta 182 (2015) 1177–1186.
[9] M. Sun, J. Feng, Y. Bu, et al., Highly sensitive copper fiber-in-tube solid-phase microextraction for online selective analysis of polycyclic aromatic hydrocarbons coupled with high performance liquid chromatography, J. Chromatogr. A 1408 (2015) 41–48.
[10] R. Dargahi, H. Ebrahimzadeh, R. Alizadeh, Polypyrrole coated ZnO nanorods on platinum wire for solid-phase microextraction of amitraz and teflubenzuron pesticides prior to quantitation by GC-MS, Microchim. Acta 185 (2018) 150–156.
[11] W. Bian, Z. Liu, G. Lian, et al., High reliable and robust ultrathin-layer gold coating porous silver substrate via galvanic-free deposition for solid phase microextraction coupled with surface enhanced Raman spectroscopy, Anal. Chim. Acta 994 (2017) 56–64.
[12] M. Kazemipour, M. Behzadi, R. Ahmadi, Poly(o-phenylenediamine-co-o-toluidine)/modified carbon nanotubes composite coating fabricated on a stainless steel wire for the headspace solid-phase microextraction of polycyclic aromatic hydrocarbons, Microchem. J. 128 (2016) 258–266.
[13] J. Li, Y. Liu, H. Su, et al., In situ hydrothermal growth of a zirconium-based porphyrinic metal-organic framework on stainless steel fibers for solid-phase microextraction of nitrated polycyclic aromatic hydrocarbons, Microchim. Acta 184 (2017) 3809–3815.
[14] X. Hu, C. Wang, J. Li, et al., Metal–organic framework-derived hollow carbon nanocubes for fast solid-phase microextraction of polycyclic aromatic hydrocarbons, ACS Appl. Mater. Interfaces 10 (2018) 15051–15057.
[15] L. Qiu, Q. Liu, X. Zeng, et al., Sensitive detection of bisphenol A by coupling solid phase microextraction based on monolayer graphene-coated Ag nanoparticles on Si fibers to surface enhanced Raman spectroscopy, Talanta 187 (2018) 13–18.
[16] M. Behzadi, M. Mirzaei, Poly(o-anisidine)/graphene oxide nanosheets composite as a coating for the headspace solid-phase microextraction of benzene, toluene, ethylbenzene and xylenes, J. Chromatogr. A 1443 (2016) 35–42.
[17] M. Behzadi, M. Mirzaei, M. Daneshpajooh, Carbon nanotubes/poly-ortho-aminophenol composite as a new coating for the headspace solid-phase microextraction of polycyclic aromatic hydrocarbons, Anal. Methods 6 (2014) 9234–9241.
[18] N. Alizadeh, M. Kamalabadi, A. Mohammadi, Determination of histamine and tyramine in canned fish samples by headspace solid-phase microextraction based on a nanostructured polypyrrole fiber followed by ion mobility spectrometry, Food Anal. Methods 10 (2017) 3001–3008.
[19] Y. Bu, J. Feng, X. Wang, et al., In situ hydrothermal growth of polyaniline coating for in-tube solid-phase microextraction towards ultraviolet filters in environmental water samples, J. Chromatogr. A 1483 (2017) 48–55.
[20] M. Behzadi, E. Noroozian, M. Mirzaei, Electropolymerization of carbon nanotubes/poly-ortho-aminophenol nanocomposite on a stainless steel fiber for the solid-phase microextraction of phthalate esters, RSC Adv. 4 (2014) 50426–50434.
[21] H. Asiabi, Y. Yamini, S. Seidi, et al., Electroplating of nanostructured polyaniline–polypyrrole composite coating in a stainless-steel tube for on-line in-tube solid phase microextraction, J. Chromatogr. A 1397 (2015) 19–26.
[22] A. Amiri, Solid-phase microextraction-based sol–gel technique, TrAC Trends Anal. Chem. 75 (2016) 57–74.
[23] Dj. Djozan, M. Amir-Zehni, Copper sulfide wire as a selective fiber in solid-phase microextraction, Chromatographia 58 (2003) 221–224.
[24] M.A. Farajzadeh, M. Hatami, A new selective SPME fiber for some n-alkanes and its use for headspace sampling of aqueous samples, J. Sep. Sci. 26 (2003) 802–808.
[25] Y. Liu, Y. Shen, M.L. Lee, Porous layer solid phase microextraction using silica bonded phases, Anal. Chem. 69 (1997) 190–195.
[26] M. Behzadi, E. Noroozian, M. Mirzaei, Electrodeposition of a copolymer nanocomposite for the headspace solid-phase microextraction of benzene, toluene, ethylbenzene and xylenes, J. Iran. Chem. Soc. 15 (2018) 1391–1398.
[27] K. Molaei, H. Bagheri, A.A. Asgharinezhad, et al., SiO_2-coated magnetic graphene oxide modified with polypyrrole–polythiophene: a novel and efficient nanocomposite for solid phase extraction of trace amounts of heavy metals, Talanta 167 (2017) 607–616.
[28] H.M. Marwani, E.Y. Danish, M.A. Alhazmi, et al., Cellulose acetate-iron oxide nanocomposites for trace detection of fluorene from water samples by solid-phase extraction technique, Separ. Sci. Technol. 53 (2018) 887–895.
[29] X. Liang, R. Ma, L. Hao, et al., β-Cyclodextrin polymer@Fe_3O_4 based magnetic solid-phase extraction coupled with HPLC for the determination of benzoylurea insecticides from honey, tomato, and environmental water samples 41 (2018) 1539–1547.
[30] M. Hesampour, M.A. Taher, M. Behzadi, Synthesis, characterization and application of a $MnFe_2O_4$@poly(o-toluidine) nanocomposite for magnetic solid-phase extraction of polycyclic aromatic hydrocarbons, New J. Chem. 41 (2017) 12910–12919.
[31] M. Bhattacharya, Polymer nanocomposites—a comparison between carbon nanotubes, graphene, and clay as nanofillers, Materials 9 (2016) 262–297.
[32] I. Sapurina, Y. Li, E. Alekseeva, et al., Polypyrrole nanotubes: the tuning of morphology and conductivity, Polymer 113 (2017) 247–258.
[33] Y. Shi, L. Pan, B. Liu, et al., Nanostructured conductive polypyrrole hydrogels as high-performance, flexible supercapacitor electrodes, J. Mater. Chem. A 2 (2014) 6086–6091.
[34] T.F. Otero, S. Beaumont, Chemical sensors from the cooperative actuation of multistep electrochemical molecular machines of polypyrrole: voltammetric study, Sens. Actuators B Chem. 253 (2017) 958–966.
[35] Y. Wang, Y. Qiu, Z. Chen, et al., Corrosion of polypyrrole: kinetics of chemical and electrochemical processes in NaOH solutions, Corros. Sci. 118 (2017) 96–108.
[36] R.A. Green, N.H. Lovell, L.A. Poole-Warren, Impact of co-incorporating laminin peptide dopants and neurotrophic growth factors on conducting polymer properties, Acta Biomater. 6 (2010) 63–71.
[37] W. Xu, A. Palumbo, J. Xu, et al., On-Demand capture and release of organic droplets using surfactant-doped polypyrrole surfaces, ACS Appl. Mater. Interfaces 9 (2017) 23119–23127.
[38] S. Bhandari, N.K. Singha, D. Khastgir, Synthesis of graphene-like ultrathin polyaniline and its post-polymerization coating on nanosilica leading towards superhydrophobicity of composites, Chem. Eng. J. 313 (2017) 1302–1310.
[39] O. Ballesteros, A. Zafra, A. Navalon, et al., Sensitive gas chromatographic–mass spectrometric method for the determination of phthalate esters, alkylphenols, bisphenol A and their chlorinated derivatives in wastewater samples, J. Chromatogr. A 1121 (2006) 154–162.
[40] X.-L. Cao, Determination of phthalates and adipate in bottled water by headspace solid-phase microextraction and gas chromatography/mass spectrometry, J. Chromatogr. A 1178 (2008) 231–238.
[41] A. Mousa, C. Basheer, A.R. Al-Arfaj, Application of electro-enhanced solid-phase microextraction for determination of phthalate esters and bisphenol A in blood and seawater samples, Talanta 115 (2013) 308–313.
[42] M.A. Moreira, L.C. André, Z.L. Cardeal, Analysis of plasticiser migration to meat roasted in plastic bags by SPME–GC/MS, Food Chem. 178 (2015) 195–200.
[43] Q. Liu, D. Chen, J. Wu, et al., Determination of phthalate esters in soil using a quick, easy, cheap, effective, rugged, and safe method followed by GC–MS, J. Sep. Sci. 41 (2018) 1812–1820.
[44] L. Correia-Sá, S. Norberto, C. Delerue-Matos, et al., Micro-QuEChERS extraction coupled to GC–MS for a fast determination of Bisphenol A in human urine, J. Chromatogr. B 1072 (2018) 9–16.